SURFACE FATIGUE: A COMPARISON BETWEEN ZrO_2 AND CaF_2.

M.-O. Guillou*, C. Maerky*, J.L. Henshall† and R.M. Hooper*

Repeated point contact loading has been used to investigate the surface fatigue deformation and fracture of ZrO_2 and CaF_2 single crystals, which both have the fluorite crystal structure. The soft impressor method is described and the observed surface fatigue effects are presented and discussed. Since zirconia is much harder than CaF_2, the contact pressures required to develop observable fatigue effects were correspondingly higher. In both cases, cracking was observed to occur in the (001) test planes much earlier than it appeared in the (111) test planes. Fatigue cracks in ZrO_2 are initiated via a dislocation interaction mechanism, whereas cleavage cracks are observed in CaF_2.

INTRODUCTION

The soft impressor method has proven to be a successful technique to investigate the accumulation of deformation and fatigue initiated cracks in a number of ceramic materials. The reasons for using this test method, and the details of the technique, have been described elsewhere (Guillou et al (1-3)). The purpose of the work reported herein is to compare the surface fatigue behaviour of two single crystal ceramic materials, calcia stabilized zirconia and calcium fluoride, which have been chosen since they both have the fluorite crystal structure and also {001}<110> slip system at room temperature. However, the bonding in zirconia is less ionic than that of fluorspar (≈50% vs 80% respectively). Table 1 summarises the properties of ZrO_2 and CaF_2.

EXPERIMENTAL PROCEDURE

All tests were performed in air at room temperature using a purpose built computer

---

* School of Engineering, University of Exeter, Exeter, U.K.
† Department of Mechanical Engineering, University of Brunel, Uxbridge, U.K.

controlled apparatus, as shown schematically in Figure 1 (1–3). Briefly, the soft impressor technique is based on repeated point contact loading of a flat, polished ceramic surface, by using a nominally sharp 120° conical tip of a softer deformable material. The fatigue effect is produced by sinusoidally varying the applied load at a frequency of about 2Hz. The primary advantages of using this type of surface fatigue test are that the plastic deformation of the metallic cone during the initial loading cycle results in good alignment of the two contacting surfaces and the stress state has been characterised (unlike conventional hardness testing).

The ceramic test surfaces were flat, polished ($\leq$ 1/4 µm diamond) (001) and (111) planes of both 14mol% CaO stabilized ZrO_2 (Ca-CSZ) and CaF_2. The metallic impressors used were hardened silver steel (BS1407:1970, heat treated for one hour at 850°C and oil quenched), and magnesium silicon containing aluminium alloy (BS1474:1972) for testing Ca-CSZ and CaF_2 respectively. The ceramic substrate to metallic tip hardness ratio was $\approx$ 1.5. The cyclic load conditions applied were 19.6 ± 9.8 N to test zirconia and 9.8 ± 4.9 N for calcium fluoride, which respectively resulted in a maximum applied pressure of 6.8 GPa and 0.8 GPa over the measured circular contact areas.

RESULTS AND DISCUSSION

(001) planes of CaF_2 and ZrO_2. Figure 2 shows the effect of repeated point contact loading on the cube plane of both crystals. The CaF_2 specimen was etched to reveal the extent of plastic deformation. The dislocation rosette increased in size with increasing number of cycles to its full expansion ($\approx$ 3.5 times the diameter of the contact zone) after 10^5 cycles (Fig. 2b). Both the initiation of a ring crack at the edge of the contact zone and a radial crack were observed after 10^4 cycles (Fig. 2a). Further cycling did not have a significant influence on crack propagation (Fig 2b). There is no effective dislocation etchant at room temperature for zirconia. However, confocal microscopy demonstrated that plastic deformation occurred in ZrO_2 beneath the impressor, leading to residual shallow impressions (1–5 µm deep). No discernible fracture was optically visible for tests performed up to 10^3 cycles on the Ca-CSZ substrate. A thin crack was observed to propagate at the edge of the contact zone after 2.5 x 10^3 cycles. An almost full thin ring crack was obtained after 5 x 10^3 cycles (Fig. 2c). Substantial conchoidal cracking, adjacent to the contact zone, was produced as the number of cycles was increased, leading to the formation of non-crystallographic debris ($\approx$1 µm in size) together with metal adhesion (Fig. 2d).

(111) planes of CaF_2 and ZrO_2. The extent of the etch-pits around impressions performed on (111) CaF_2 is slightly greater than that observed on the (001) plane (Fig. 3a). However no cracking was observed for a number of cycles as high as

10^5. Three fine sharp cracks along $<1\bar{1}0>$ were observed at the edge of the contact zone after 10^6 cycles (Fig. 3b), but no radial cracks were visible. In ZrO_2, cracking initiated at the edge of the contact zone after 6 x 10^4 cycles and extended to a full ring crack after 9 x 10^4 cycles with three pronounced sites approximately along $<1\bar{1}0>$ (Fig. 3c). Subsurface cracking was also observed adjacent to the contact area. With increasing number of cycles the fracture mode became mainly conchoidal, leading to extensive damage and metal transfer (Fig. 3d).

For both ZrO_2 and CaF_2, the (001) plane is more susceptible to fatigue damage than the (111) plane. In all cases, cracking was generally observed to initiate at the edge of the contact zone, where the tensile stresses are maximum. For both materials, no crystallographic fracture occurred in the cube plane, while the three $<1\bar{1}0>$ directions were preferred for cracks to initiate in the (111) plane. For ZrO_2, cracking was initiated in {110} crack planes by a dislocation interaction mechanism $(a/2[01\bar{1}]_{(100)}+a/2[110]_{(010)}\rightarrow a/2[110]_{(1\bar{1}0)})$, whereas for CaF_2, cleavage cracking would appear to occur preferentially. Although zirconia is slightly tougher than calcium fluoride, fracture occurred at a later stage in the latter. Also, once a crack had initiated in ZrO_2, its rate of propagation was very rapid and led to conchoidal fragmentation and considerable fatigue damage. This was not observed in CaF_2 in which cracks barely propagated with increasing number of cycles.

CONCLUSION

The results of the present investigation clearly indicate that both ZrO_2 and CaF_2 are susceptible to cyclic fatigue under point contact loading. The soft impressor technique provides controlled plastic deformation and cracking in these two isostructural ceramic materials. Both CaCSZ and CaF_2 exhibit greater crack resistance on (111) than (001), by a factor of >10 times. Crack initiation in CaCSZ is followed by surface fragmentation, whereas in CaF_2 there was very limited crack extension.

REFERENCES

(1) Guillou, M.-O., Henshall, J.L. and Hooper, R.M., J. Am. Ceram. Soc., Vol. 76, No.7, 1993, pp.1832-1836.

(2) Guillou, M.-O., Henshall, J.L. and Hooper, R.M., Wear, Vol. 170, 1993, pp. 247-253.

(3) Guillou, M.-O., Henshall, J.L. and Hooper, R.M., J. Mater. Sci., Vol. 30, 1995, pp. 151-161.

Materials	14 mol% CaO stabilized ZrO_2	CaF_2
Degree of ionicity	50%	80%
Elastic constants (GPa)		
C_{11}	410	164
C_{12}	110	53
C_{44}	60	34
Knoop hardness† (GPa)		
(001)	10.3 – 11.5	1.6 – 1.8
(111)	10.4 – 11.2	1.6 – 1.7
Indentation fracture toughness† (MPa.m$^{1/2}$)		
(001)	0.6 – 1.2	0.6 – 0.8
(111)	1.5 – 2.0	0.9 – 1.0
Bond strength (kJ/mol)	762	523

† Applied load 29.4 N, dwell time 12 seconds.

TABLE 1 – A summary of the properties of ZrO_2 and CaF_2.

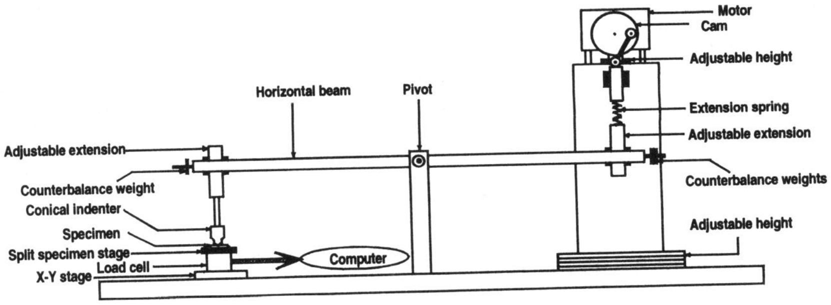

Figure 1 A schematic illustration of the cyclic fatigue apparatus.

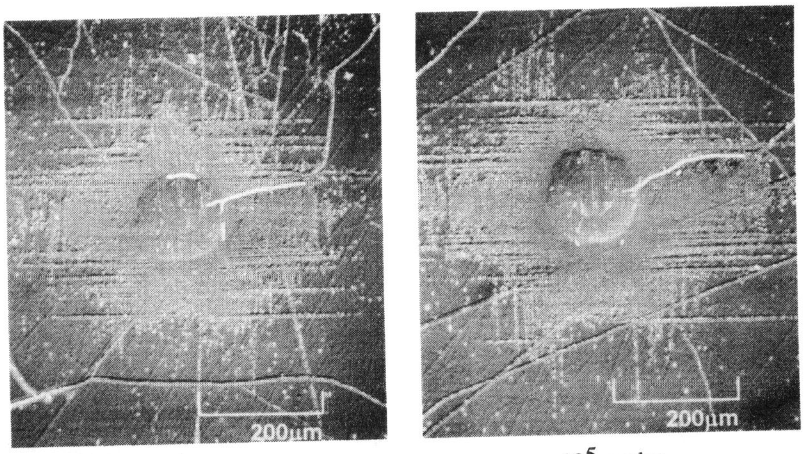

10^4 cycles

→ [100]

(a)

10^5 cycles

→ [100]

(b)

Figure 2 (a & b) (001) CaF_2 - Cyclic load: 9.8 ± 4.9 N.

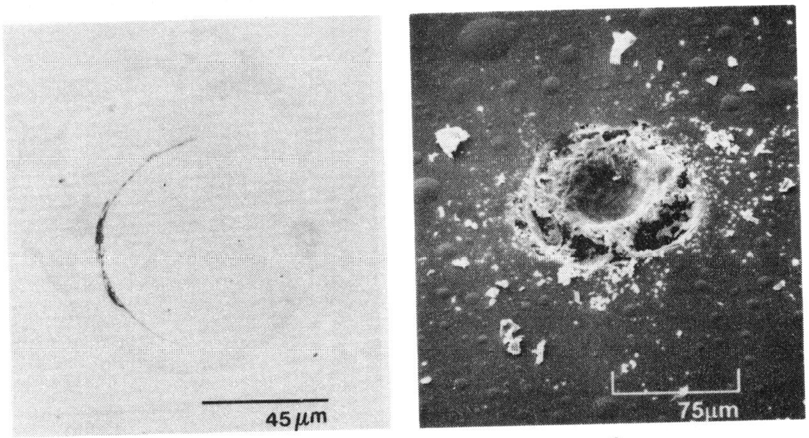

5 x 10^3 cycles

↑ [110]

(c)

25 x 10^3 cycles

(d)

Figure 2 (c & d) (001) Ca-CSZ - Cyclic load: 19.6 ± 9.8 N.

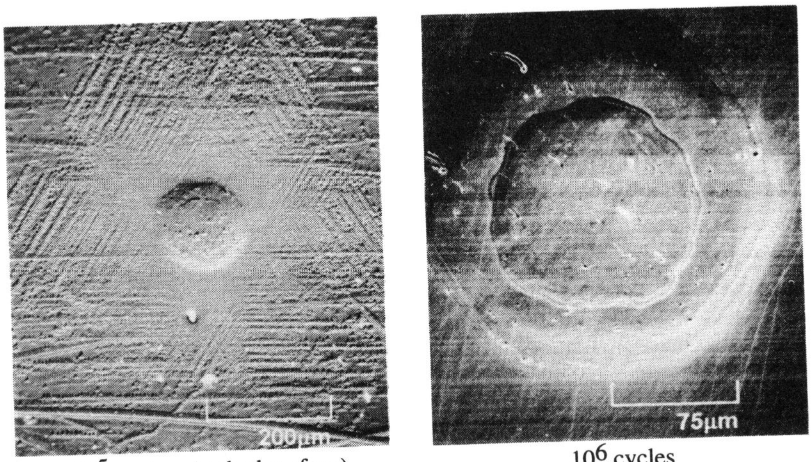

10^5 cycles (etched surface)

→ $[1\bar{1}0]$

(a)

10^6 cycles

→ $[1\bar{1}0]$

(b)

Figure 3 (a & b) (111) CaF_2 – Cyclic load: 9.8 ± 4.9 N.

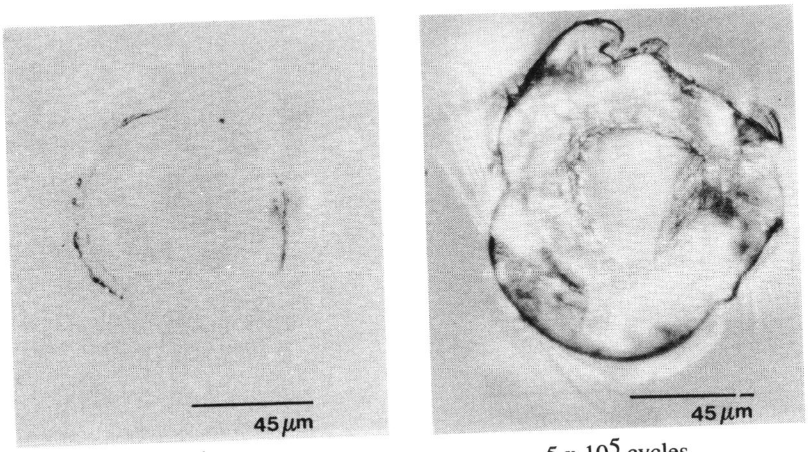

9 x 10^4 cycles

↑ $[1\bar{1}0]$

(c)

5 x 10^5 cycles

↑ $[1\bar{1}0]$

(d)

Figure 3 (c & d) (111) Ca-CSZ – Cyclic load: 19.6 ± 9.8 N.